Diametral error correction in turning slender workpieces: an integrated approach

Diametral error correction in turning slender workpieces: an integrated approach

Diametral Error Correction in Turning Slender Workpieces: An Integrated Approach

Niccolò Grossi*, Antonio Scippa, Gianni Campatelli

Department of Industrial Engineering, University of Florence, Via di Santa Marta 3, 50139, Firenze, Italy

*Corresponding author. Tel.: +39- 055-2758726; E-mail address: niccolo.grossi@unifi.it

Abstract

Turning slender components is a critical task since workpiece flexibility entails relevant deformations during the process, leading to potential loss of accuracy, lower machining efficiency and higher manufacturing costs. In this paper a compensation strategy for diametral error in turning of slender workpieces is presented. The proposed method computes a toolpath that compensate diametral error based on the prediction of such error performed by a Finite Element based approach. The developed algorithm automatically generates the compensated toolpath based on few inputs: nominal toolpath, workpiece material, tool geometry, stock dimensions and fixturing system. First, nominal toolpath is analyzed and discretized, then at each step workpiece deflection is estimated by coupling the FE model of the workpiece (automatically generated using Timoshenko beam elements) and the cutting forces model. Material removal is considered in the process by updating the geometry of the stock at each step of the machining cycle. Using the predicted deformation of the workpiece the compensated toolpath is generated and the toolpath ISO-standard file is updated. The proposed algorithm was experimentally validated on four case studies: three single diameter bars and a multi-diameter shaft. The results demonstrate the accuracy of the proposed predictive approach, with small deviations in estimating average diametral error (less than 6 μm). Furthermore, it has been demonstrated that the compensated toolpath is successful in reducing the diametral errors by at least 50%, as well as smoothing the error shape, confirming that providing an accurate prediction of the shape error could represent an effective approach for its reduction. The proposed methodology could form the basis of a toolpath simulation and optimization software, useful for machining shops that deals with slender shafts turning.

Keywords: Turning; Tool path; Stiffness; Diametral error; Compensation.

1. Introduction

Manufacturing slender axisymmetric components is still a challenging task even with modern machining processes [1]. Due to its adaptability and the achievable high quality (i.e., surface roughness and geometrical/dimensional precision), the turning process stands out as the primary technology to manufacture such components. Demanding standards for quality, however, frequently contrast with feasible production rates. Determining an appropriate machining cycle is therefore essential to achieving the right balance between those two factors. Surface roughness is primarily influenced by cutting parameters (e.g., feed rate) and tool geometry, but geometrical errors are also induced by the compliance of the workpiece. The deflection caused by cutting forces affects the actual depth of cut, introducing form errors that may result in scraps or unacceptable defects [2]. Creating a machining cycle based on both the component stiffness and the cutting forces (i.e., the cutting parameters and workpiece material) is necessary to minimize geometrical errors while retaining high productivity. The simplest strategy that may be used to attain such a goal is based on trial-and-error techniques, which frequently reflect in increased lead times. Additionally, this strategy becomes less acceptable when batch size lowers and material cost rises, and it does not guarantee the selection of an optimal solution, which can only be achieved by predicting the workpiece behavior during the process. Two are the main detrimental effects in machining high-compliance workpieces: i) chatter vibrations and ii) deflections.

Chatter, a self-excited vibration phenomenon, significantly affects surface finish, tool life, and overall productivity [3]. Chatter in turning has been widely studied [4]. Prediction of such instability is one of the major investigated aspects [5]: Urbikain et al. proposes two methods, a traditional single frequency model and a modern collocation method based on Chebyshev polynomials integrated with multimode analysis, to predict chatter in large horizontal lathes [6]. Focusing on slender workpieces, the same authors addresses chatter prediction in straight turning using the same stability model developed through the Chebyshev collocation method [7], while Sekar et al. [8] proposes an analytical approach through a compliance model for the chatter stability analysis in turning, focusing on tailstock-supported workpieces. A similar work was proposed by Lu et al. [9] examining the effect of cutting tool movement along the workpiece's length on chatter stability. In addition, special turning process are also investigated: Wan et al. [10] proposed a method to study the dynamic behavior of rotational truncated conical thin-walled workpieces during turning, Nam et al. [11] introduced the first analytical chatter stability prediction for low-frequency vibration-assisted turning and Beri et al. [12] investigated chatter prediction in the turning process of slender workpieces by applying time-periodic axial loads as suppression method. Indeed, chatter suppression is a promising approach to deal with this detrimental effect [13].

Even in case chatter is prevented, dynamic and static workpiece compliance could cause high deflections leading to unacceptable errors. One of the widely adopted solutions is predicting such error by using a cutting force mechanistic model combined with workpiece behavior modeling strategy [14]. In milling, due to its inherent characteristics both static [15] and dynamic [16] effects should be considered [17], while in turning static effects are most prominent since cutting force are theoretically constant, and generally lead to diametral errors.

Several works have been dedicated to diametral error prediction in turning of slender shafts. Giorleo et al. [18][19] proposed an analytical formulation for slender workpiece based on beam theory for single diameter turning, and later they extend such an approach to multi-diameter condition [20]. Their work considers the most adopted constraint solutions (i.e., cantilever, between-centers, chuck-center) and highlights the importance of considering shearing effect on the beam modeling. Jianliang and Rongdi [21] proposes a similar model, including the follow rest configuration and considering a statistical model for cutting forces.

In order to consider more complex shape, finite difference approach [22] and finite element method [23] were applied to diametral error prediction. Finite element method could be an interesting approach to increase the level of complexity and accuracy of the workpiece models, as also demonstrated by the applications to turning of thin-walled parts [24] and tool deflection prediction in milling [2,25]. Recently Bergs et al. [26] proposed to adopt the segmentation method to predict diametral error, including the influence of tool wear.

Since all these works were focused on finishing, in most of them material removal was neglected. Although keeping diametral error inside tolerance is a requirement of finishing operations, uniformity of machining allowance in roughing could be critical for the subsequent finishing operations. Compensating diametral error along the entire machining cycle (i.e., roughing and finishing) could be exploited to avoid the need of additional phases (e.g., semi-finishing). In such scenario, as shown by Kops et al. [27], it is important to consider material removal (i.e., emerging diameter) during the process for an accurate prediction of the diametral error, at least when depth of cut is over 2 mm. In Kops et al. work a method to take this effect into account based on analytical formulations was developed, limited to single diameter bars. In addition to numerical/analytical approaches, Artificial Neural Networks (ANN) were also applied to diametral error prediction: Wang and Zhang [28] proposed to train a neural network with hybrid genetic algorithm for the purpose, while Benardos et al. [29] developed both a numerical model using a stored energy formulation and an ANN-based approach.

Once the diametral error is predicted, compensation strategy should be developed, as proposed for milling by López de Lacalle et al. [14]. However, few works are dedicated to compensating diametral error in turning of slender workpieces and most of them are based on experimental or neural network results instead of physic-based models, increasing the number of experiments required. Topal and Ço□un [30] proposed a compensation strategy based on an empirical model, while Suneel and Pande [31] used ANN to generate compensated toolpath. Li and Du [32] combined different error sources for their compensation strategy but for force-induced error they still rely on ANN.

To reduce the number of experiments, the physic-based predictive models described above could be exploited but most of them lack the capability of automatically compute diametral error with a minimum set of parameters and directly analyzing and generating toolpaths, considering multiple passes and workpiece complex shapes.

This work presents an automatic solution for turning of flexible components with the purpose of generating toolpaths to minimize geometrical errors, compensating the workpiece deflection. The proposed approach combines all the required features for a comprehensive analysis, prediction, and compensation of diametral error in turning of slender workpieces.

Compared to the other approaches found in literature the proposed method:

i) is based on finite element Timoshenko beam models, including the shearing effect, and allowing the accurate prediction of complex shape bars behavior.
ii) Considers material removal of the stock, essential in roughing operations, by updating the workpiece geometry at each machining step.
iii) Starts directly from the programmed toolpath (i.e., G-Code) and it considers the evolution of the diametral error for different operations and tools, multiple passes, and hence multi-diameter configurations.
iv) Automatically analyzes the nominal toolpath, computes the diametral error, and provides a compensated toolpath without the need of additional parameters.

At the core of the proposed approach is the innovative concept of seamlessly incorporating a predictive model for workpiece deflection compensation. This integration enables the computation of toolpaths to account for variations in workpiece compliance throughout the turning process, influenced by material removal and the instantaneous cutting conditions. The proposed methodology forms the basis for the implementation of a software for machining shops to reduce experimental trial and error procedures and achieve first-right-time manufacturing on turning of slender workpieces. The proposed approach does not require additional inputs from the operator and uses simplified models to simulate the process, compute cutting forces, and predict deflection and diameter of the component. The optimized toolpath can be directly imported into a CNC lathe, reducing diametral error.

First, the paper presents the proposed approach, describing the different blocks in which is composed. The numerical analyses involved in the toolpath optimization process are simplified to make their automation feasible and time effective. Cutting forces are estimated using a mechanistic force model. Workpiece behavior is modeled using Finite Element Method (Timoshenko beam element), its generation and update during the machining process are automatic, only toolpath and stock geometry are needed. Second, experimental validation is presented, specific tests were carried out of simplified case studies focusing on roughing operations, where geometrical errors are relevant, and the machined geometry could affect the subsequent phases (i.e., semi-finishing and finishing). Finally, conclusions are drawn, and future activities described.

2. Proposed approach

The proposed predictive approach can be summarized in Fig. 1. At the background level, the proposed algorithm includes a toolpath analyzer module that will read the ISO standard program (i.e., G-Code), identifying cutting parameters and distinguishing the different passes. For each pass the toolpath is discretized, and workpiece behavior simulated through the interface between workpiece FE and cutting force model using a static analysis.

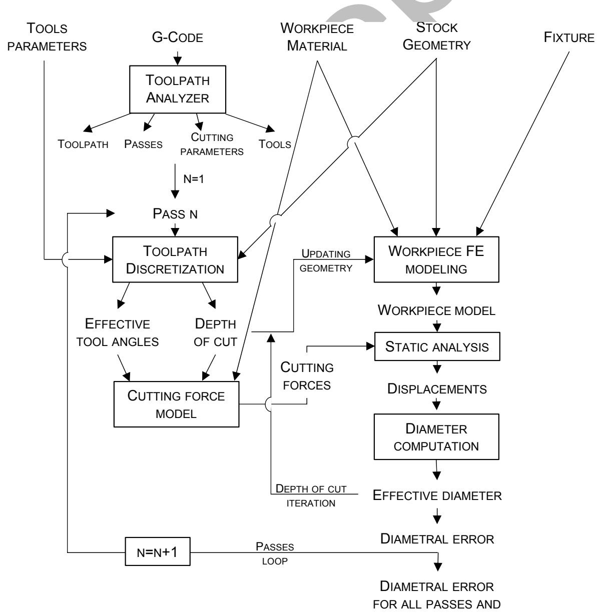

Fig. 1 General overview of the predictive algorithm

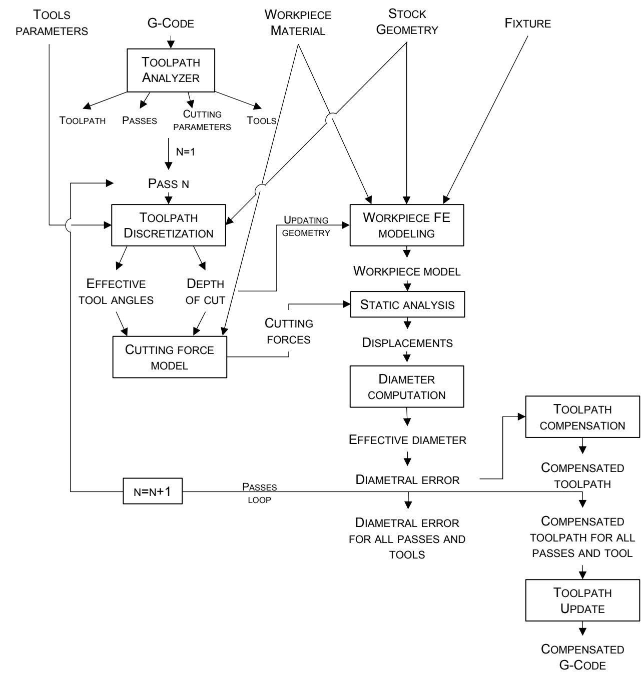

Fig. 2 General overview of the compensation algorithm.

Material removal is considered by updating the workpiece geometry at each step. Diametral error is evaluated by comparing the expected diameter (i.e., the one commanded in the G-Code) with the computed one. Compensation strategy starts from such prediction, as schematized in Fig. 2. Diametral error is used to modify the toolpath that is then written in the G-Code format and used to update the original G-Code. The main difference between prediction and compensation in the diametral error definition is the depth of cut iteration, as detailed below, and outlined in the flowchart in Fig. 3

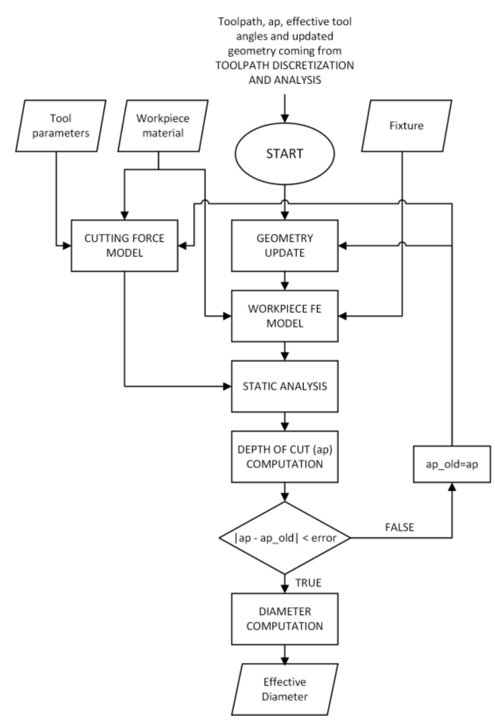

Fig. 3 Detailed flowchart of the depth of cut iteration

One of the innovative ideas underpinning the proposed approach is to fully integrate the workpiece deflection predictive model, so that the toolpath computation can be performed considering workpiece compliance changing during the turning process, as effect of material removal, and the instantaneous cutting conditions. The developed algorithm is implemented for X-Z traditional external turning.

2.1 Inputs

The proposed approach requires the following inputs, generally known by a turning shop operator:

- Nominal toolpath (G-Code)
- Stock geometry (2D representation)
- Tool geometry
- Workpiece material
- Fixture configuration

The toolpath and the stock are used to compute and update the actual geometry of the workpiece and estimate the actual depth of cut. Toolpath is input as a standard ISO code (i.e., G-Code), from which the system extracts the actual toolpath and the cutting parameters (i.e., tool number, cutting velocity and feed). Stock geometry is included as a text file, written in a specific format: starting from tailstock (or free end) of the workpiece the segments with continuous radius variation along the axis are identified. Each segment is characterized by outer and inner radius at both its ends and by its length, hence every line of the text file represents one segment. Text file is reporting five different values for each line: initial outer radius, initial inner radius, final outer radius, final inner radius, length of the segment. This approach allows to represent any axisymmetric workpiece geometry. Portion inside the chuck should not be included in this representation.

In addition to these two inputs, fixture configuration, tool geometry and workpiece material data are required. Fixture configuration (cantilever, between-centers, chuck-center) should be defined, in addition stiffness values of the constraints are required. Fixture configuration has a major impact on the diametral error, e.g., switching from cantilever to double support scheme drastically increase the stiffness of the workpiece, hence reducing the overall error. Different fixture configurations are considered in the proposed methodology as detailed in section 2.4.

For the tool, lead angle and corner radius are needed. Indeed, tool geometry affect cutting forces as detailed in section 2.3.

The workpiece material elastic material proprieties (i.e., Elastic Modulus and Poisson Ratio) and cutting force coefficients should be input. The firsts are required for workpiece compliance estimation, while cutting force coefficients are used to predict cutting forces.

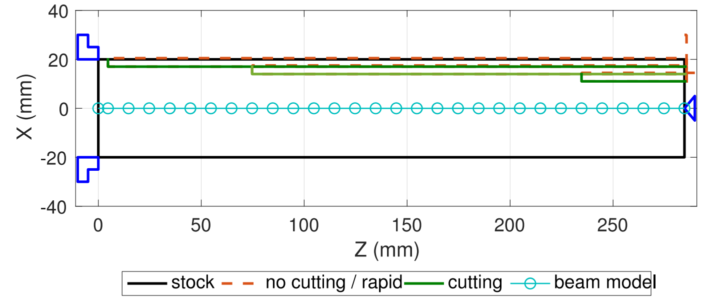

Fig. 4 Stock and toolpath example.

2.2 Toolpath analysis

Starting from the G-Code the algorithm derives the toolpath in the X-Z plane and divide the tool motion in the different passes and operations (i.e., tool changes) by identifying the single commands, as shown in Fig. 4. Each pass is then analyzed separately. The toolpath is discretized to analyze the process with the desired resolution, in this operation the actual lead angle is estimated based on the feed direction and the actual depth of cut is extracted based on the workpiece geometry.

2.3 Cutting force model

The cutting force model implemented in the proposed approach, and already adopted in other works [33,34], is provided below:

$$F_t = K_{tc}bh + K_{te}b \qquad F_{rf} = K_{rfc}bh + K_{rfe}b$$

$$F_f = F_{rf}\cos(\Omega) \qquad F_{ap} = F_{rf}\sin(\Omega)$$

where F_t is the cutting force in the cutting speed direction, while F_{rf} on the rake face plane, decomposed in feed force (F_f) and depth of cut force (F_{ap}), K_{ic} are the cutting force coefficients and K_{ie} the edge coefficients, b is the contact length and h is the chip thickness, Ω is the chip flow angle. Cutting force coefficients for the specific material can be easily experimentally derived (e.g., using the procedure reported by Altintas [1]) or taken from literature. Such coefficients can be then used for different cutting and tool parameters by exploiting the specific chip flow angle that can be computed from the actual lead angle, corner radius of the tool, actual depth of cut and feed by just using a geometrical formulation. The Colwell approximation for such angle was used in this work [35]. Analyzing forces formulations (eq. 1-2), the influence of tool geometry and turning cutting parameters on cutting forces can be highlighted. Two are the main contributions of tool geometry: first, tool geometry (especially rake angles) will affect cutting force coefficients, hence the magnitude of the total cutting forces; second, tool geometry (i.e., corner radius, lead angle) will affect the chip flow angle (computed in this work with the Colwell approximation) hence the cutting force direction, altering the magnitude of F_{ap}, main responsible for diametral error. The main cutting parameters affecting cutting forces are depth of cut and feed, since they directly influence b and h in the cutting force equation. This cutting force model was selected for its simplicity that eases the implementation of the proposed methodology and subsequent industrial implementation. Alternatively, the proposed approach allows for the incorporation of a more complex cutting force model, which could encompass additional factors like tool wear or be customized for specific machining strategies [36]. This simply involves changing the cutting force formulations and adding the necessary extra parameters.

2.4 Workpiece FE modeling and analysis

Workpiece deflection is estimated by applying the predicted cutting forces on a FE model of the component. Since slender workpieces are the target of the proposed approach Timoshenko beam 1D model [37] was selected as modeling strategy. A dedicated algorithm was implemented starting from the workpiece geometry and material to create nodes distribution (i.e., mesh) and element stiffness matrices, then assembled in the unconstrained component stiffness matrix K (Fig. 4). At each machining step the geometry is updated, and stiffness matrix reconstructed.

Constrained stiffness matrix is obtained by considering boundary conditions of chuck and tailstock (if present). In this work constraints are not considered rigid, therefore a 6x6 diagonal stiffness matrices are adopted as follows:

$$K_{chuck} = diag(K_{xc}, K_{yc}, K_{zc}, K_{rotxc}, K_{rotyc}, K_{rotzc}) \quad (1)$$

$$K_{tail} = diag(K_{xt}, K_{yt}, K_{zt}, K_{rotxt}, K_{rotyt}, K_{rotzt}) \quad (2)$$

where diag() is the diagonal matrix that is characterized on its diagonal by the values provided in the bracket and K_{ij} are the stiffness value on the i degree of freedom for the j constraint. K_{chuck} is then assembled to the unconstrained matrix K by adding such matrix to the last node, while K_{tail}, if present, is assembled to the first node (i.e., end of the workpiece). The boundary condition model adopted is simplified and does not consider the full machine tool behavior and/or other type of errors (e.g., assembly error [38]). However, such a model is the most adopted solution in case static deflection of slender workpiece is investigated, and it was the starting point for the development of the proposed methodology. More complex boundary condition model, especially for tailstock, could be developed and included in the framework, valid in general.

2.5 Geometry updating

The proposed workpiece modeling procedure allows to consider emerging diameter and material removal by updating the workpiece geometry at each time step, based on the tool position and actual depth of cut. The tool positions are analyzed in the toolpath analyzer to determine if the tool is cutting or not. For each cutting position geometry is analyzed: if required, a new section is added to the geometry and geometry is updated with the actual radius generated by the tool, as shown in the example of single diameter bar of Fig. 5. Such geometry update allows to create a node on the FE model of workpiece, applying the predicted cutting forces to such node, the workpiece deflection is estimated by performing static analysis.

Such an approach is repeated for each cutting position of the toolpath. An iterative approach was used to consider the actual workpiece geometry and depth of cut: first the deflection was estimated using the commanded depth of cut, such first-attempt deflection was used to update both workpiece geometry and depth of cut, and a new deflection was evaluated, such cycle was repeated until convergence (i.e., minimization of the error on predicted deflections). Two iterations were often enough to reach convergence.

2.6 Diameter and error prediction

Workpiece deflections estimated via static analysis on workpiece model are used to compute the effective machined geometry (i.e., the effective workpiece diameter, D_{eff}) as proposed in [18] and written for the specific case in the following equation:

$$D_{eff} = 2\sqrt{(X - dx)^2 + dy^2}$$

where X is the commanded motion of the tool (i.e., desired radius), dx is the deflection on depth of cut direction and dy is the deflection on the cutting direction.

2.7 Toolpath compensation

As shown in Fig. 2, toolpath compensation is carried out following the same approach of the predictive algorithm, adding at the end the compensation procedure. The only difference between the two predictive parts is related to the depth of cut iteration, not used in the compensation algorithm.

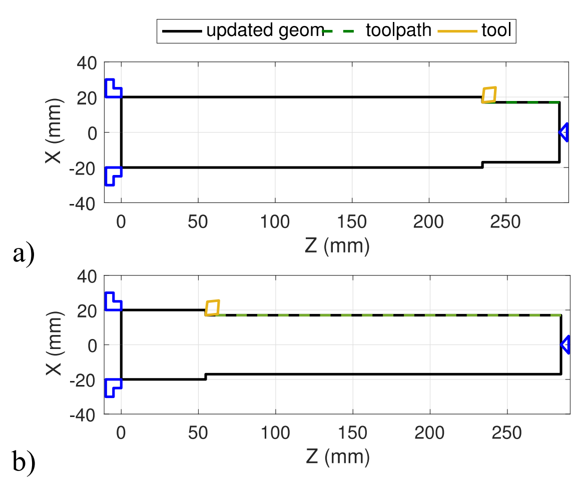

Fig. 5 Geometry update a) time step i b) time step i+a

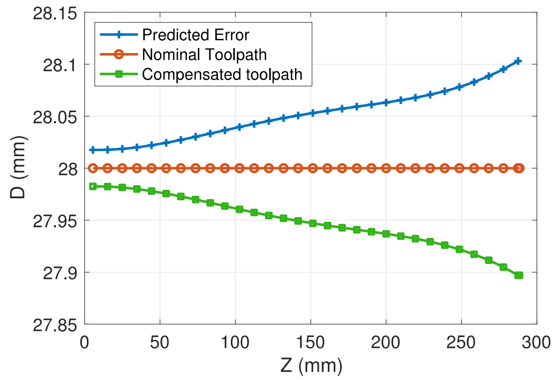

Fig. 6 Example of compensated toolpath

This is because, in case of compensated toolpath, desired depth of cut becomes constant and there is no need to consider the depth of cut variation. Such an approach removes the need of depth of cut iteration in the compensation algorithm, improving its efficiency. Based on the effective workpiece diameter, a new toolpath is derived and written in a new file using ISO standard, an example is provided in Fig. 6. In such procedure only the motion commands (i.e., X, Z) of the G-Code are modified, keeping the basis of the compensated program equal to the input one.

2.8 Integration

The different modules are integrated by exchanging data as highlighted in Fig. 1 and Fig. 2. The proposed approach was implemented in MATLAB. Timoshenko beam FE models are constructed and solved inside the algorithm without the need of an external FE solver.

3. Experimental results

An experimental validation of the proposed approach was performed on a Mori Seiki SL-2500Y CNC lathe (Fig. 7) in an industrial facility (humidity around 55-60%, ambient temperature around 20° C [39,40]).

a)

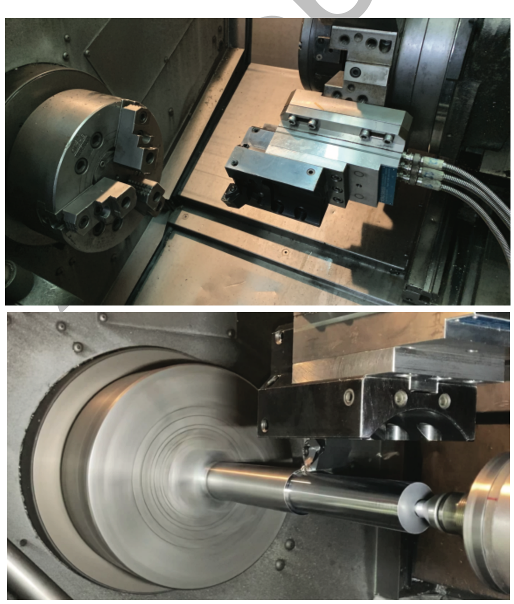

b)

Fig. 7 a) experimental set-up b) turning of a case study.

Table 1 Tool parameters

Rake angle [°]	Relief angle [°]	Lead angle [°]	Corner radius [mm]
14	6	-5	0.8

Different workpiece geometries were tested, using the same tool and material: C45 Steel. C45 Steel was selected as common material for components that could represent a potential industrial application of the proposed methodology, such as shafts for general applications. Indeed, C45 as a high-strength medium-carbon steel, can achieve good mechanical properties (e.g., higher strength and toughness) after quenching and tempering (or normalizing), while keeping cost low.

A Sandvik Coromant CNMG 120408-PM 4425 insert was used, installed on a T-Max toolholder P DCLNL 2525M 12. Tool parameters, considering the insert mounted on the toolholder, are provided in Table 1.

Four case studies were machined starting from a cylindrical stock of 40 mm diameter. Three simple single diameter cylinders (analyzing a single pass) and one shaft with three different diameters (analyzing three subsequent passes), their geometries are shown in the figures (Fig. 8, Fig. 9, Fig. 10, Fig. 11). For all the case study, chuck-center fixture configuration was used (i.e., chuck and tailstock). In the experimental validation double support scheme was used since it is the most adopted solution in case of slender workpieces.

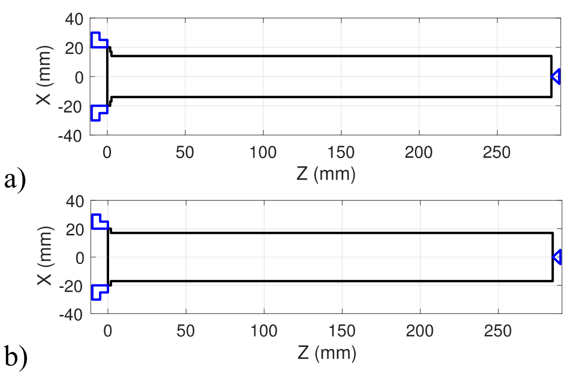

Fig. 8 Case A (overhang 287.5 mm) a) stock D: 34 mm b) final D: 28 mm.

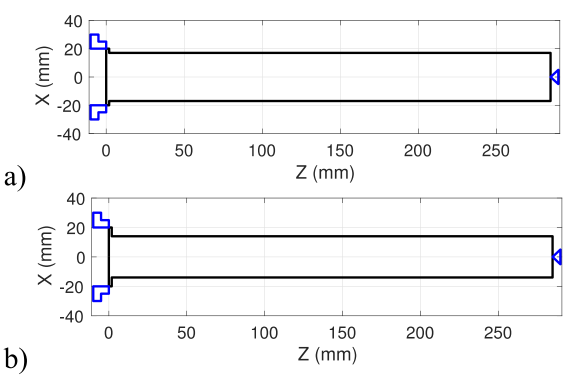

Fig. 9 Case B (overhang 287.5 mm) a) stock D: 28 mm b) final D: 24 mm.

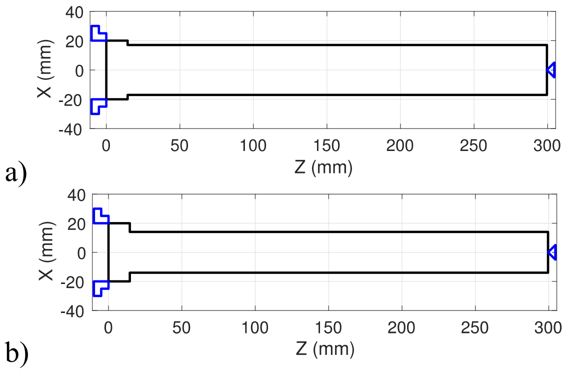

Fig. 10 Case C (overhang 299.5 mm) a) stock D: 34 mm b) final D: 28 mm.

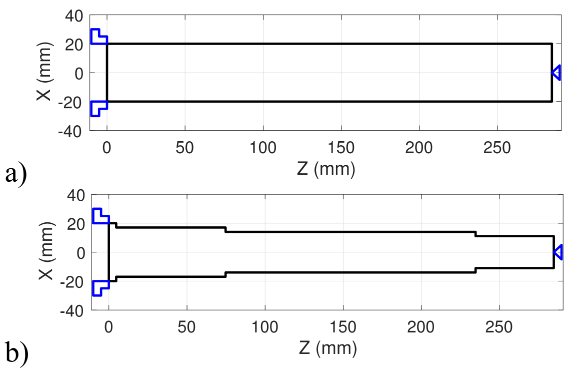

Fig. 11 Shaft (overhang 287.5 mm) a) stock D: 40 mm b) after 1st pass D: 34 mm L: 280 mm, 2nd pass D: 28 mm L: 210 mm and final pass D: 22 mm L: 50 mm.

Table 2 Cutting parameters

Cutting velocity v_c [m/min]	Feed f [mm/r]	Depth of cut a_p [mm]
200	0.2	2 (case study B) 3 (case study A-C-shaft)

Table 3 Cutting force coefficients

K_{tc} [MPa]	K_{te} [N/mm]	K_{rfc} [MPa]	K_{rfe} [N/mm]
1748.5	99.2	703.0	92.5

Roughing operations were investigated with the cutting parameters provided in Table 2.

3.2 Cutting forces

Cutting force prediction was carried out using cutting force coefficients identified for the specific tool-material couple performing preliminary tests. Cutting forces were acquired by a Kistler 9257A table dynamometer and the procedure proposed by Altintas [1] was used to extract cutting force coefficients. Results, summarized in Table 3, show values in line with the ones found in literature [41].

3.3 Workpiece model

Before testing the proposed methodology, experimental modal analysis was performed to identify material properties and constraints stiffness. No sensitivity analysis on such parameters was carried out.

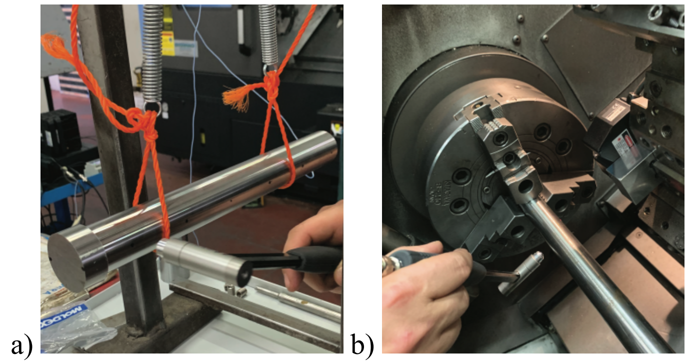

Fig. 12 Impact testing a) free-free condition b) constrained

Table 4 Constraints stiffnesses

	Kx / Ky [N/mm]	Kz [N/mm]	K rotx / K roty [N mm/rad]	K rotz [N mm/rad]
Chuck	3.30e4	1e15	6.87e7	3e7
Tail	5.50e3	1e15	0	0

This would allow the proposed approach to be assessed without such uncertainties. Material properties were identified by using free-free modal analysis through impact testing (Fig. 12a). Typical steel values were derived: Young Modulus: 210150 MPa, Poisson Ration: 0.28. Furthermore, chuck and tailstock stiffnesses were calculated by means of experimental modal analysis in the constrained configurations (Fig. 12b). The tailstock was represented as a pinned end (i.e., free rotations) and the chuck as a fixed end. Stiffness values are provided in Table 4. Results for chuck are in accordance with values reported in previous publications [19], while tailstock stiffness values are lower than expected: the machine tool used for the tests features a high-compliant tailstock system.

3.4 Prediction results

A comparison of predicted and measured diametral errors was carried out to examine the effectiveness of the proposed method in estimating the machined workpiece geometry. After manufacturing, diameters of the different case studies were measured by means of digital micrometer MAHR Micromar 40ER with 1 μm of resolution. Measurement uncertainty (i.e., error limit) of the measuring instrument is 2 μm. Measurements were repeated five times with very small deviations between the different measurements (around 1-2 μm), hence the average value was presented. Such results were compared with proposed approach outcomes, obtained by using a mesh size and a toolpath discretization of 10 mm. Using such parameters simulations last about 5s for the first three cases and 6s for the shaft on a laptop (2.4 GHz Dual-Core Intel Core i5, 8 GB RAM). Simulations were performed with and without considering material removal. Fig. 13 shows the results for all the case studies.

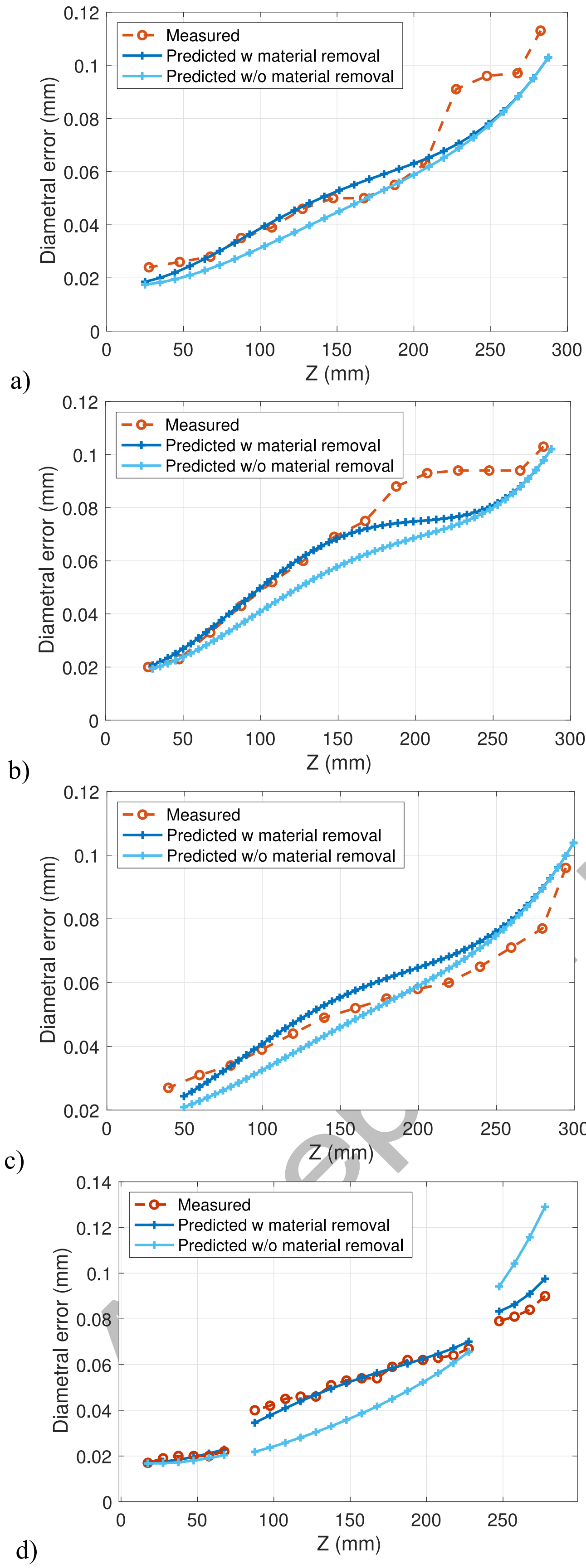

Fig. 13 Comparison between predicted and measured diametral errors: a) case study A, b) case study B, c) case study C, d) shaft.

Comparison between the predictive approach results (including material removal) and experiments show good agreement, especially in terms of overall error difference between tailstock and chuck (average deviation on predicting the errors of 6.0, 5.4, 4.7, 4.1 μm in case studies A, B, C and shaft respectively). However, certain differences in the error shape are found, most likely because of the tailstock modeling. It is important to note that the tailstock stiffness in the investigated conditions is a key factor in determining the error shape. Indeed, maximum error is found to be similar for all the case studies (about 0.1 mm) and it is located at the tailstock end.

In addition, analyzing results with and without material removal it is possible to highlight the importance of the including such effect, both in terms of error shape and magnitude. Indeed, the proposed predictive approach demonstrates significantly higher accuracy compared to the version that excludes material removal. In case of single diameter bars (Fig. 13a,b,c) the need of material removal algorithm is crucial to achieve an accurate representation of the error in the mid part of the cylinders. This is because in that region workpiece has already significantly change its geometry (i.e., diameter) and cutting forces are still located on a high-compliance zone. As expected, case study B is the more influenced by considering material removal, since such case study presents higher L/D ratio (i.e., 12).

In case of multi-passes (Fig. 13d) this influence is even more prominent. Indeed, in this case the material removal plays a crucial role since the workpiece drastically changes its shape during the process. As expected, the differences between prediction with and without material removal are very high analyzing the final pass: at the tailstock about 0.03 mm difference is found.

3.5 Toolpath compensation

The proposed methodology was subsequently applied to calculate the compensated toolpath by considering material removal in all the case studies, following the algorithm presented in Fig. 2.

Geometries were machined using both the compensated and non-compensated toolpaths to assess the improvement achieved by the proposed approach. Results, shown in Fig. 14, clearly indicate that the compensated toolpath effectively reduces errors, at least halving the maximum error and smoothing the shape. The average reductions were approximately 62%, 58%, 70%, and 60% for case studies A, B, C, and the shaft, respectively.

The overall error is well-compensated except in the vicinity of the tailstock. Indeed, using the compensated toolpath, diametral error was maintained under 0.02 mm in the region 0-250 mm from the chuck for case C and shaft, 0.04 mm for case A and B, while using the nominal toolpath the error reached over 0.08 mm in the same region.

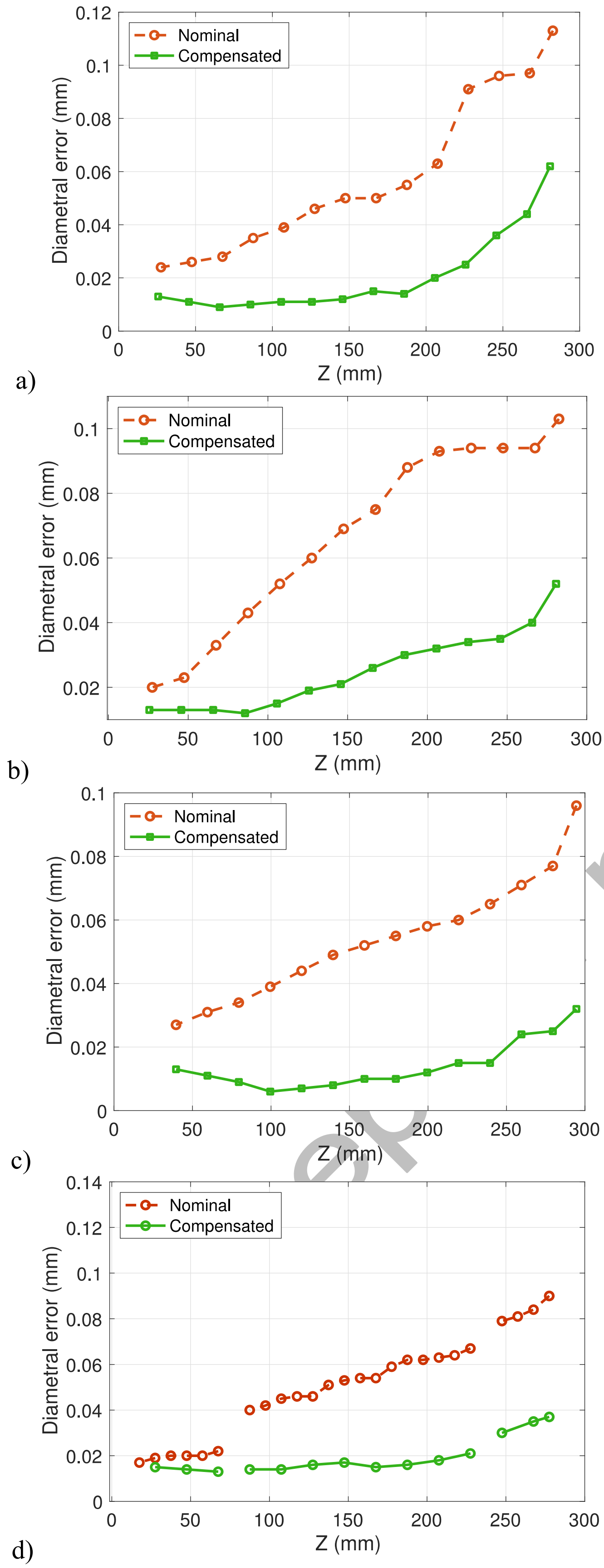

Fig. 14 Comparison between measured diametral errors with and without compensation strategy: a) case study A, b) case study B, c) case study C, d) shaft.

On the other hand, approaching the tailstock the compensation algorithm fails in keeping the error under control, since the error increases to 0.06 mm in case A and B and 0.04 mm for case C and shaft. However, in the same region (250-300 mm from the chuck), without compensation significant higher error was obtained (over 0.1 mm for all case study).

This decrease of performance of the compensation algorithm is probably due to local effects of tailstock constraints and non-modeled impacts of cut entry. Further investigation is needed to enhance the solution in these areas. Nevertheless, even near the tailstock, significant reductions were achieved: approximately 45% for case A, 53% for B, 67% for C, and 59% for the shaft. Moreover, in all the cases investigated compensation never impact negatively on the diameter accuracy, always representing an improvement in the quality of the product.

Conclusions

This work presents a tailored approach for the computation of toolpaths to compensate diametral error in turning of slender workpieces.

The following conclusions can be drawn:

- The prediction of workpiece deflection, based on simplified FE model and cutting forces estimation, has shown to be adequately accurate in estimating the overall shape errors, with small deviations in estimating average diametral error, less than 6 μm for all the case studies.
- Material removal is essential to achieve an accurate representation of the diametral error both in terms of shape and magnitude, especially for multi-passes cutting cycle.
- Such predictive approach was exploited to compute the compensated toolpath and results confirm that providing an accurate prediction of the shape error could represent an effective approach for its reduction. Compensated toolpath significantly reduces diametral error for on all the case studies with an average reduction between 58% and 70%, as well as smoothing the error shape.
- The proposed approach still needs an accurate representation of the boundary conditions (i.e., fixture stiffnesses), experimentally derived in this work.

The experimental validation shows that the error is globally reduced by at least 50% compared to the non-compensated tests. Such results were consistent for all the case studies investigated. Although some residual errors could be highlighted approaching the tailstock, the proposed approach seems promising in drastically reducing the shape error in roughing operations which could be exploited to avoid the need of semi-finishing phases. Even at the tailstock a reduction between 45% and 67% of the diametral error is achieved.

Further activities will be focused on investigating alternative constraints modeling strategy for the tailstock to considering local effects and improve the prediction accuracy, including machine tool influence on stiffness and assembly errors [38]. Moreover, the proposed approach will be applied to finishing operations to study its effectiveness in such scenario. Finally, a procedure to indirectly estimate fixture stiffness without the need of dedicated experimental approaches will be investigated.

Once refined, the proposed methodology could find useful application in machining shop in which turning of slender workpieces is adopted, allowing to reduce experimental trial and error procedures and achieve a first-right-time manufacturing. Since the proposed approach is based on simplified models (e.g., mechanistic cutting forces, workpiece as a beam, boundary condition model), it can be easily implemented in a software that starting from inputs already known by the operator (i.e., stock material and geometry, traditional toolpath, tool geometry and machine characteristics) simulates the process and compute actual depth of cut and cutting forces. These first data are already interesting for the user, simulating the toolpath could be useful for detecting anomalies, programming errors and collisions. Predicted cutting forces can be then applied to the workpiece FE beam model to predict deflection and hence diameter of the final geometry. If such geometry is not compliant with the desired one (i.e., tolerances), compensated toolpath can be computed. The optimized toolpath is written in standard ISO language and can be directly imported in the CNC lathe to machine the selected component, reducing the resulting diametral error.

Acknowledgements

This research was developed within the DRITTO project, funded as an experiment of DIH-World, an Horizon2020 project (grant agreement 952176). The authors wish to thank all the project partners. The support of Lorenzo Sallese and Marco Ceccarelli of Meccanica Ceccarelli e Rossi s.r.l. is gratefully acknowledged.

References

[1] Y. Altintas, Manufacturing Automation: Metal Cutting Mechanics, Machine Tool Vibrations, and CNC Design, (2012).

[2] Y. Altintas, O. Tuysuz, M. Habibi, Z.L. Li, Virtual compensation of deflection errors in ball end milling of flexible blades, CIRP Ann. 67 (2018) 365–368. doi:10.1016/j.cirp.2018.03.001.

[3] U. Bravo, O. Altuzarra, L.N. López De Lacalle, J.A. Sánchez, F.J. Campa, Stability limits of milling considering the flexibility of the workpiece and the machine, Int. J. Mach. Tools Manuf. 45 (2005) 1669–1680. doi:10.1016/J.IJMACHTOOLS.2005.03.004.

[4] M. Siddhpura, R. Paurobally, A review of chatter vibration research in turning, Int. J. Mach. Tools Manuf. 61 (2012) 27–47. doi:10.1016/J.IJMACHTOOLS.2012.05.007.

[5] G. Urbikain, D. Olvera, L.N.L. de Lacalle, A. Beranoagirre, A. Elías-Zuñiga, Prediction methods and experimental techniques for chatter avoidance in turning systems: A review, Appl. Sci. 9 (2019). doi:10.3390/APP9214718.

[6] G. Urbikain, F.J. Campa, J.J. Zulaika, L.N. López De Lacalle, M.A. Alonso, V. Collado, Preventing chatter vibrations in heavy-duty turning operations in large horizontal lathes, J. Sound Vib. 340 (2015) 317–330. doi:10.1016/J.JSV.2014.12.002.

[7] G. Urbikain, L.N. López De Lacalle, F.J. Campa, A. Fernández, A. Elías, Stability prediction in straight turning of a flexible workpiece by collocation method, Int. J. Mach. Tools Manuf. 54–55 (2012) 73–81. doi:10.1016/J.IJMACHTOOLS.2011.11.008.

[8] M. Sekar, J. Srinivas, K.R. Kotaiah, S.H. Yang, Stability analysis of turning process with tailstock-supported workpiece, Int. J. Adv. Manuf. Technol. 43 (2009) 862–871. doi:10.1007/S00170-008-1764-2/METRICS.

[9] K. Lu, Z. Lian, F. Gu, H. Liu, Model-based chatter stability prediction and detection for the turning of a flexible workpiece, Mech. Syst. Signal Process. 100 (2018) 814–826. doi:10.1016/J.YMSSP.2017.08.022.

[10] M. Wan, H.N. Wang, Y. Yang, Dynamics of the truncated conical thin-wall turning process, J. Manuf. Process. 94 (2023) 49–62. doi:10.1016/J.JMAPRO.2023.03.059.

[11] S. Nam, B. Eren, T. Hayasaka, B. Sencer, E. Shamoto, Analytical prediction of chatter stability for modulated turning, Int. J. Mach. Tools Manuf. 165 (2021) 103739. doi:10.1016/J.IJMACHTOOLS.2021.103739.

[12] B. Beri, G. Meszaros, G. Stepan, Machining of slender workpieces subjected to time-periodic axial force: stability and chatter suppression, J. Sound Vib. 504 (2021) 116114. doi:10.1016/J.JSV.2021.116114.

[13] J. Munoa, X. Beudaert, Z. Dombovari, Y. Altintas, E. Budak, C. Brecher, et al., Chatter suppression techniques in metal cutting, CIRP Ann. 65 (2016) 785–808. doi:10.1016/J.CIRP.2016.06.004.

[14] L.N. López de Lacalle, A. Lamikiz, M.A. Salgado, S. Herranz, A. Rivero, Process planning for reliable high-speed machining of moulds, Int. J. Prod. Res. 40 (2002) 2789–2809. doi:10.1080/00207540210140068.

[15] L. Morelli, N. Grossi, A. Scippa, G. Campatelli, Extended classification of surface errors shapes in peripheral end-milling operations, J. Manuf. Process. 71 (2021) 604–624. doi:https://doi.org/10.1016/j.jmapro.2021.09.054.

[16] L. Morelli, N. Grossi, G. Campatelli, A. Scippa, Surface location error prediction in 2.5-axis peripheral milling considering tool dynamic stiffness variation, Precis. Eng. 76 (2022) 95–109. doi:10.1016/J.PRECISIONENG.2022.03.008.

[17] S. Herranz, F.J. Campa, L.N.L. De Lacalle, A. Rivero, A. Lamikiz, E. Ukar, et al., The milling of airframe components with low rigidity: A general approach to avoid static and dynamic problems, Proc. Inst. Mech. Eng. Part B J. Eng. Manuf. 219 (2005) 789–801. doi:10.1243/095440505X32742.

[18] L. Carrino, G. Giorleo, W. Polini, U. Prisco, Dimensional errors in longitudinal turning based on the unified generalized mechanics of cutting approach. Part I: Three-dimensional theory, Int. J. Mach. Tools Manuf. 42 (2002) 1509–1515. doi:10.1016/S0890-6955(02)00117-7.

[19] L. Carrino, G. Giorleo, W. Polini, U. Prisco,

Dimensional errors in longitudinal turning based on the unified generalized mechanics of cutting approach. Part II: Machining process analysis and dimensional error estimate, Int. J. Mach. Tools Manuf. 42 (2002) 1517–1525. doi:10.1016/S0890-6955(02)00117-7.

[20] G. Giorleo, W. Polini, U. Prisco, Machining errors in turning of a multi-diameter workpiece, in: D.T. Pham, E.E. Eldukhri, A.J. Soroka (Eds.), Proc. Innov. Prod. Mach. Syst., Cardiff, Uk, 2014.

[21] G. Jianliang, H. Rongdi, A united model of diametral error in slender bar turning with a follower rest, Int. J. Mach. Tools Manuf. 46 (2006) 1002–1012. doi:10.1016/j.ijmachtools.2005.07.042.

[22] L.Z. Qiang, Finite difference calculations of the deformations of multi-diameter workpieces during turning, J. Mater. Process. Technol. 98 (2000) 310–316. doi:10.1016/S0924-0136(99)00267-8.

[23] M. Lee, C. Lee, Development of analysis model for geometric error in turning processes, J. Cent. South Univ. 18 (2011) 711–717. doi:10.1007/s11771-011-0752-0.

[24] H. Manikandan, T.C. Bera, A turning simulation environment for geometric error estimation of thin-walled parts, Int. J. Adv. Manuf. Technol. 119 (2022) 789–809. doi:10.1007/s00170-021-08298-3.

[25] M. Soori, B. Arezoo, M. Habibi, Tool Deflection Error of Three-Axis Computer Numerical Control Milling Machines, Monitoring and Minimizing by a Virtual Machining System, J. Manuf. Sci. Eng. 138 (2016). doi:10.1115/1.4032393.

[26] T. Bergs, D. Knappe, K. Husseini, T. Pullen, D. Schraknepper, J.E. Döring, Investigation of the diameter error when turning thin walled workpieces, Procedia CIRP. 102 (2021) 343–348. doi:10.1016/j.procir.2021.09.059.

[27] L. Kops, M. Gould, M. Mizrach, Improved analysis of the workpiece accuracy in turning, based on the emerging diameter, J. Manuf. Sci. Eng. Trans. ASME. 115 (1993) 253–257. doi:10.1115/1.2901657.

[28] W. Gang, H.Z. Wei, Prediction of diameter error of workpiece in turning process using neural network, 2009 Int. Conf. Intell. Human-Machine Syst. Cybern. IHMSC 2009. 1 (2009) 95–98. doi:10.1109/IHMSC.2009.32.

[29] P.G. Benardos, S. Mosialos, G.C. Vosniakos, Prediction of workpiece elastic deflections under cutting forces in turning, Robot. Comput. Integr. Manuf. 22 (2006) 505–514. doi:10.1016/j.rcim.2005.12.009.

[30] E.S. Topal, C. Ço□un, A cutting force induced error elimination method for turning operations, J. Mater. Process. Technol. 170 (2005) 192–203. doi:10.1016/j.jmatprotec.2005.05.003.

[31] T.S. Suneel, S.S. Pande, Intelligent tool path correction for improving profile accuracy in CNC turning, Int. J. Prod. Res. 38 (2000) 3181–3202. doi:10.1080/002075400418216.

[32] X. Li, R. Du, Analysis and compensation of workpiece errors in turning, Int. J. Prod. Res. 40 (2002) 1647–1667. doi:10.1080/00207540110100685.

[33] L. Croppi, N. Grossi, A. Scippa, G. Campatelli, Fixture optimization in turning thin-wall components, Machines. 7 (2019). doi:10.3390/machines7040068.

[34] F. Atabey, I. Lazoglu, Y. Altintas, Mechanics of boring processes - Part I, Int. J. Mach. Tools Manuf. 43 (2003) 463–476. doi:10.1016/S0890-6955(02)00276-6.

[35] L. V Colwell, Predicting the Angle of Chip Flow for Single-Point Cutting Tools, Trans. Am. Soc. Mech. Eng. 76 (2022) 199–203. doi:10.1115/1.4014795.

[36] F.J. Amigo, G. Urbikain, L.N. López de Lacalle, O. Pereira, P. Fernández-Lucio, A. Fernández-Valdivielso, Prediction of cutting forces including tool wear in high-feed turning of Nimonic® C-263 superalloy: A geometric distortion-based model, Measurement. 211 (2023) 112580. doi:10.1016/J.MEASUREMENT.2023.112580.

[37] A. Ertürk, H.N. Özgüven, E. Budak, Analytical modeling of spindle–tool dynamics on machine tools using Timoshenko beam model and receptance coupling for the prediction of tool point FRF, Int. J. Mach. Tools Manuf. 46 (2006) 1901–1912. doi:10.1016/j.ijmachtools.2006.01.032.

[38] E. Díaz-Tena, U. Ugalde, L.N. López De Lacalle, A. De La Iglesia, A. Calleja, F.J. Campa, Propagation of assembly errors in multitasking machines by the homogenous matrix method, Int. J. Adv. Manuf. Technol. 68 (2013) 149–164. doi:10.1007/S00170-012-4715-X/METRICS.

[39] M.Ş. ADİN, Performances of cryo-treated and untreated cutting tools in machining of AA7075 aerospace aluminium alloy, Eur. Mech. Sci. 7 (2023) 70–81. doi:10.26701/EMS.1270937.

[40] M.Ş. Adin, Machining aerospace aluminium alloy with cryo-treated and untreated HSS cutting tools, Adv. Mater. Process. Technol. (2023) 1–26. doi:10.1080/2374068X.2023.2273035.

[41] D. Śniegulska-Gradzka, M. Nejman, K. Jemielniak, Cutting Force Coefficients Determination Using Vibratory Cutting, Procedia CIRP. 62 (2017) 205–208. doi:10.1016/j.procir.2016.06.091.

Statements and Declarations

Funding: This research was funded by DIH-World, an Horizon2020 project (grant agreement 952176), within the DRITTO experiment.

Competing Interests: The authors have no relevant financial or non-financial interests to disclose.

Author contributions: Conceptualization, N.G. and A.S.; methodology, N.G..; software, N.G.; validation, N.G. and A.S.; investigation, N.G.; writing—original draft preparation, N.G.; writing—review and editing, N.G. and G.C.; project administration, N.G. and G.C.; supervision, G.C.